and K_m is absorbed as a scale factor. With this configuration, knowledge of the numerical magnitude of K_m is no longer required.

It will be noted that the various forms of the expression are symmetrical in respect of K_1 and K_2 so that, as far as the polarization ratio is concerned, the question of whether it is an *ante*-monochromator or a *post*-monochromator arrangement (Mathieson, 1968) is not, in that respect, critical.

In an operational sense, the relative sequence of the monochromator and specimen crystals may lead to differences. Where only relative values of intensities are sought, there is virtually no distinction. If, however, absolute intensities are the aim, there is an advantage in the case of the *ante*-monochromator (case I, Mathieson, 1968). With this configuration, one can measure the intensity of the beam incident on the specimen crystal, since that is monochromated, and the polarization factor for the specimen crystal alone is

$$P_s = \frac{(1 + K_m)[1 + K_s(2\theta)]}{1 + K_m} = 1 + K_s(2\theta).$$

In conclusion, it is interesting to note that although Kirkpatrick (1927) made an observation, in a similar vein, concerning how to deal with the possibility of the X-rays from an X-ray tube being polarized, its significance for the use of monochromator crystals has not apparently been commented on over the last half-century.

References

CHANDRASEKHAR, S., RAMASESHAN, S. & SINGH, A. K. (1969). *Acta Cryst.* A**25**, 140–142.

FURNAS, T. C. & BEARD, D W. (1965). Am. Crystallogr. Assoc. Summer Meet., Gatlinburg. Abstr. p. 18.

INTERNATIONAL UNION OF CRYSTALLOGRAPHY (1978). *Acta Cryst.* A**34**, 159–160.

KIRKPATRICK, P. (1927). *Phys. Rev.* **29**, 632–636.

MATHIESON, A. McL. (1968). *Rev. Sci. Instrum.* **39**, 1834–1837.

MATHIESON, A. McL. (1977). *Acta Cryst.* A**33**, 133–136.

OLEKHNOVICH, N. M., RUBTSOV, V. A. & SHMIDT, M. P. (1975). *Kristallografiya*, **20**. 796–802. [Engl. Trans. *Sov. Phys. Crystallogr.* (1975). **20**, 488–491.]

Acta Cryst. (1978). A**34**, 406–413

Interaction Energies at Twin Boundaries and Effects of the Dihedral Reentrant and Salient Angles on the Growth Morphology of Twinned Crystals

BY R. BOISTELLE

Centre de Recherche sur les Mécanismes de la Croissance Cristalline, CNRS, Centre de Saint-Jérôme, 13397 *Marseille CEDEX* 4, *France*

AND D. AQUILANO

Istituto di Mineralogia, Cristallografia e Geochimica dell' Università di Torino, via S. Massimo 24, 10123 *Torino, Italy*

(*Received* 22 *October* 1977; *accepted* 26 *November* 1977)

Twin-boundary energies are calculated with the Lennard-Jones 6–12 potential function for the (110) and (310)-twin laws of orthorhombic even *n*-alkane crystals. In agreement with experiment, the calculations show that the higher the interaction energy along the twin boundary, the higher the probability of observing the corresponding twin. According to the values of the reentrant angles, the adsorption sites near the twin boundary may act as permanent growth sites (kinks) where growth takes place spontaneously and leads to a crystal elongated in the direction of the twin boundary.

1. Introduction

A peculiar aspect of the growth of twinned crystals showing dihedral reentrant and salient angles is the change of the normal growth kinetics of the faces which form these angles. Generally, the occurrence of a reentrant angle is followed by an increase of the growth kinetics; this phenomenon was observed on different crystalline species (Frank, 1949; Stranski, 1949). To our knowledge, no kinetic measurements have been

carried out and the explanations which have been proposed (Frank, 1949; Hartman, 1956) are mainly qualitative. Two hypotheses were considered in order to explain the effect of the reentrant angle on the growth kinetics. According to Frank (1949) it is the lattice of screw dislocations generated at the twin boundary which starts a permanent advancement of the faces in the reentrant angle since the line where they meet belongs to the twin boundary. According to Hartman (1956) the twin boundary is a permanent step if the faces which build it up are *F* faces, or *S* faces if their zone axis is not parallel to the twin boundary. In both cases, the faces of the reentrant angle can grow without two-dimensional nucleation, since the permanent step provides the existence of kinks at which the crystal growth takes place. Finally, there are no explanations about the behaviour of the twins in the region of the salient angle, nor about the dependence of the change in the growth kinetics upon the values of the reentrant angle.

The growth kinetics of twinned crystals showing reentrant or salient angles are mainly assumed to be diffusion dependent. On the other hand, the adhesion energies of the molecules adsorbed on the crystal are rarely taken into account. The aim of this paper is to show in what manner these adhesion energies can influence the growth of some crystal faces as a function of the position of the adsorbed molecules, especially in the region of the dihedral reentrant angle of a twin, and to evaluate the influence of the value of these angles on the adhesion energies of molecules placed in the same position with respect to the twin boundary. For this study, we have chosen the long-chain even *n*-alkanes, C_nH_{2n+2}, the orthorhombic polymorphs of which often present twinned crystals. The (110) twin law was often observed for *n*-$C_{100}H_{202}$ (Dawson, 1952), *n*-$C_{94}H_{190}$ (Khoury, 1963), *n*-$C_{36}H_{74}$ (Keller, 1961) and *n*-$C_{34}H_{70}$ (Amelinckx, 1956*a*,*b*), whereas the (310) twin law was observed only for *n*-$C_{94}H_{190}$ (Khoury, 1963) and then rarely.

2. Structural features of the crystals

The long-chain even *n*-alkanes may crystallize in the orthorhombic polymorph if certain conditions are fulfilled: $n_c \geq 26$ (Smith, 1953), material not quite pure (Ubbelhode, 1938) or crystallization from some peculiar solvents (Teare, 1959). The crystals are generally rhombic flakes with well developed (001) faces limited by ⟨110⟩ edges. The value of the acute angle χ of the lozenge is theoretically 67·52° but deviations of ±2° are often observed.

The key structure is that of hexatriacontane, *n*-$C_{36}H_{74}$ (Teare, 1959), and the structures of all the members of the orthorhombic series can be derived by the method of Nyburg & Potworowski (1973). The crystals are built up of paraffinic layers, parallel to (001) and inside the layers the paraffinic chains run along [001] (Fig. 1). The space group is $Pca2_1$ with $Z = 4$. The short parameters, independent of the number of C atoms in the chain, n_c, are $a = 7{\cdot}42$ and $b = 4{\cdot}96$ Å. The parameter c is a function of n_c: $c = (2{\cdot}54n_c + 3{\cdot}693)$ Å; its value is 95·14 Å for hexatriacontane.

3. Calculation method

In order to calculate the interaction energies between the molecules, we have used the Lennard-Jones 6–12 potential function. Each C atom of the paraffinic chain is an interaction centre: a multicentre model, with n_c^2 interactions between two molecules, was employed. The potential energy of a molecule surrounded by k molecules is thus of the form:

$$U_p^\circ = \varepsilon \sum_k \sum_{i,j} \left[\frac{(r^*)^{12}}{r_{ijk}^{12}} - 2\frac{(r^*)^6}{r_{ijk}^6} \right]$$

where i and j are the numbers of C atoms in the molecules ($1 \leq i,j \leq n_c$), the sum being extended to all the k molecules. As we are dealing with hexatriacontane, $n_c = 36$. This potential function was used successfully for the calculations of interaction energies for complex monoclinic polytypes and polysynthetic twins (Aquilano, 1977; Boistelle & Aquilano, 1977) and for the calculation of heats of sublimation (Madsen & Boistelle, 1976). The force constant ε and the critical distance r^* were determined (Madsen & Boistelle, 1976) from thermodynamic data and lattice sums: ε/k

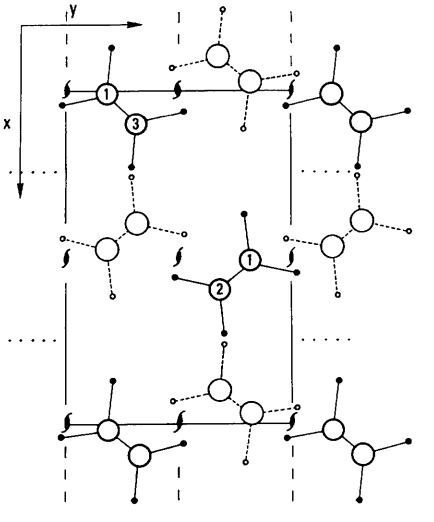

Fig. 1. (001) projection of the unit cell of orthorhombic even *n*-alkane crystals. The molecules of upper and lower layers are respectively in full and dotted lines. C(1) and C(2) are at different levels.

$= 55{\cdot}26$ K and $r^* = 4{\cdot}67$ Å. As in the sequel we are dealing with adhesion energies at room temperature, all the negative values of U_p° should be corrected by a constant positive term $\simeq 2kT$, taking into account vibrational energies (Madsen & Boistelle, 1976). However, as this correction is negligible and as we deal essentially with the interaction energy between molecules inside a layer, for which the potential energy U_p° changes linearly with n_c and can thus be extrapolated to all the members of the orthorhombic series, we prefer to give the directly computed dimensionless quantities U_p°/ε. Each unit U_p°/ε corresponds to a value of $0{\cdot}11$ kcal mol^{-1}.

4. Interaction energies in a normal orthorhombic crystal

Fig. 2 is a (001) projection of a monomolecular layer limited by (110) ledges. For the molecule adsorbed in the kink, K_N, $U_p^\circ/\varepsilon = -596$; the contributions of each molecule with respect to K_N are indicated. For a molecule adsorbed along the step, A_N, $U_p^\circ/\varepsilon = -425$, whereas for B_N the contribution of the monomolecular layer is only -52. Taking into account all the remaining molecules in the row [110], passing through A_N and B_N, U_p°/ε for the complete row [110] $= -488$, leading to $53{\cdot}72$ kcal mol^{-1}. The corresponding $\langle 110\rangle$ specific edge energy is $\gamma_{\langle 110\rangle} = 4{\cdot}185 \times 10^{-5}$ erg cm^{-1}.

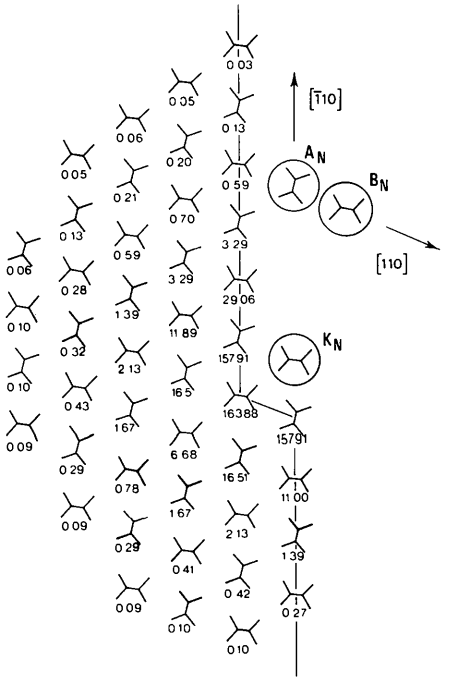

Fig. 2. Interaction energies between a molecule K_N in a kink position and its surrounding molecules inside a monomolecular layer of thickness d_{002}. Dimensionless quantities U_p°/ε.

If we consider the contribution of a complete underlying layer, not drawn in Fig. 2, on the molecule K_N, we find a value of $U_p^\circ/\varepsilon = -25$. The half-crystal energy corresponds thus to the quantity $U_p^\circ/\varepsilon = -621$. Obviously the end-packing energy (between two adjacent layers) is negligible compared with the side-packing energy (inside a layer). As the former is constant for all paraffin chain lengths, its relative importance decreases when n_c increases.

From Fig. 2 it is also possible to see in what crystallographic directions the interaction energies are the highest, in order to determine quantitatively the best periodic bond chains (p.b.c.) in the crystal (Fig. 3). According to the formalism of Hartman & Perdok (1955), it is here sufficient, for the p.b.c.'s parallel to (001), to consider those inside the monomolecular layer of thickness d_{002}. The following values have been found for a molecule placed at the end of the different rows:

Direction	⟨110⟩	[010]	[100]	⟨130⟩	[001]	⟨310⟩	⟨120⟩
$-U_p^\circ/\varepsilon$	171·53	171·48	29·82	16·93	4·00	3·29	2·23.

From these calculations, we may deduce that:

(i) the two ⟨110⟩ p.b.c.'s (the directions [110] and [$\bar{1}$10] being equivalent) and the [010] p.b.c., which run in the slice d_{002}, are built up by the strongest bonds in the structure;

(ii) the [001] p.b.c., which runs along **c**, is built up by very weak end-chain bonds;

(iii) along the directions [100], ⟨130⟩, ⟨310⟩, ⟨120⟩ we cannot find independent p.b.c.'s. As an example (Fig. 3), we may consider the slice d_{010} in which a zigzag p.b.c. runs along the [100] direction; this p.b.c. is

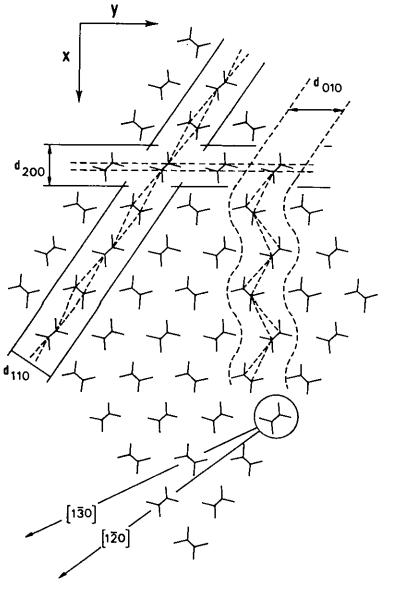

Fig. 3. Periodic bond chains in a monomolecular layer.

actually composed of elements of the ⟨110⟩ p.b.c.'s. The same consideration applies for the zigzag p.b.c.'s we may construct along the directions ⟨130⟩, ⟨310⟩ and ⟨120⟩.

We conclude that only the {001} faces have a strong F character. As for the {110} and {100} faces, which contain two p.b.c.'s (⟨110⟩, [001] and [010], [001], respectively), they have a lower F character, because of the high anisotropy between the side-packing and the end-packing energies, which means that the {001} faces may grow either by two-dimensional nucleation and/or by spiral mechanisms, whereas the {110} and {100} faces may grow by rapid filling up of rows ⟨110⟩ and [010] respectively, the growth of the rows [001] being very slow. The normal growth rates of {110} and {100} are in fact very high compared with that of {001} (Boistelle & Doussoulin, 1976; Madsen, 1978).

5. Interaction energies across the (110) twin boundary

As the interaction energies between adjacent monomolecular layers are weak and as the {110} faces contain the strongest p.b.c.'s of the crystal in the ⟨110⟩ directions, we assume in our model a flat (110) interface between the two individuals of the twin. Since in all layers the disposition of the molecules is the same, we can furthermore restrict the calculations to a twinned crystal reduced to a monomolecular layer of thickness d_{002}.

Fig. 4 is a (001) projection of such a crystal. The molecules in twin position (T) are generated by a clockwise rotation (67·52°) of the molecules of the normal crystal (N) around their [001] axis. By translation they are then shifted in such a way that the T lattice is enantiomorphous with the N lattice in regard to (110). With such an arrangement of the molecules the distances between the nearest C atoms across the twin boundary are not smaller than 4·15–4·19 Å (equilibrium distances in a normal crystal), and the distances between the corresponding H atoms (though not taken into account in our calculations) are not smaller than 2·50 Å (twice the van der Waals radius).

The interaction of O_T (Fig. 4) with the monomolecular layer N gives a value $U_p^\circ/\varepsilon = -380$. The molecule C_T which is at the centre of the unit cell of the T lattice is not in the same position as O_T with respect to the N lattice; for it $U_p^\circ/\varepsilon = -434$. These two values repeat periodically along the [110] direction; over the period $|[\bar{1}10]|$ the mean value of U_p°/ε for a 'mean' adsorbed molecule is −407. The difference between the interaction energies of this 'mean' molecule and of the normally stacked molecule (A_N in Fig. 2) corresponds to $U_p^\circ/\varepsilon = 17{\cdot}31$, *i.e.* 1·9 kcal mol^{-1}.

In order to calculate the (110) twin energy for a monomolecular layer, the contributions of the N crystal on the complete molecular rows 1 and 2 of the T crystal (Fig. 4) must be taken into account. For row 1, $U_p^\circ/\varepsilon = -500$, whereas for row 2, $U_p^\circ/\varepsilon = -444$; the interaction energy of the two rows with the crystal N is thus 51·9 kcal mol^{-1}, which corresponds, over the length $|[\bar{1}10]|$, to $8{\cdot}09 \times 10^{-5}$ erg cm^{-1}. The difference between this energy and $8{\cdot}37 \times 10^{-5}$ erg cm^{-1} ($2\gamma_{\langle 110\rangle}$ in a normal crystal) gives directly the (110) twin energy for a monomolecular layer, which is 1·82 kcal mol^{-1}, *i.e.* $0{\cdot}28 \times 10^{-5}$ erg cm^{-1}.

Thus it may be concluded that the probability of obtaining a (110) twin or a normal crystal is not too different. Furthermore, whatever the formation mechanism of such a twin, our model of the interface agrees with the observed phenomena. Effectively '... in addition to the simple (110) twinned crystals, complex crystals were frequently observed ... Although such

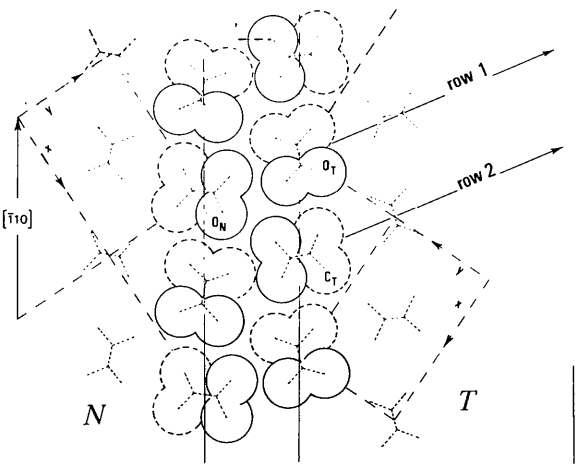

Fig. 4. (001) projection of a flat (110) twin boundary between the crystals N and T inside a monomolecular layer. H atoms: upper level (full lines), lower level (dotted lines).

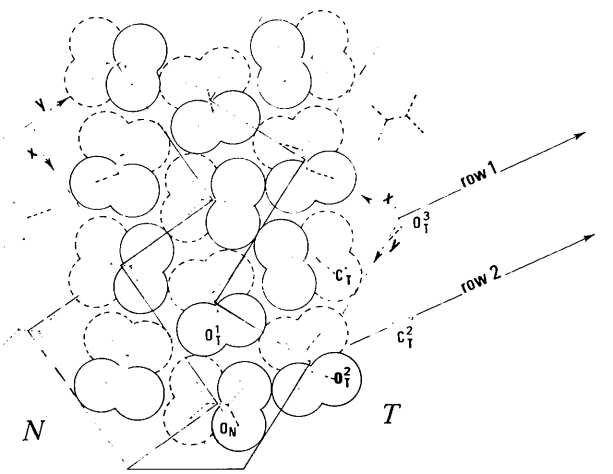

Fig. 5. (001) projection of a kinked (110) twin boundary. (Same symbols as in Fig. 4.)

aggregates often have the appearance of consisting of individual twinned crystals randomly clustered together, the geometrical relationship betweeen individuals radiating primary and secondary branches, often indicates that multiple twinning forms, are essential features of the development of many of these complex crystals' (Khoury, 1963).

The results obtained with our model of straight twin boundary can now be compared with those arising from the model of Dawson (1952) and Khoury (1963). Here (Fig. 5) the interface between the two individuals of the twin is a mean (110) plane, actually made up of (100) and (010) microfacets alternating on a period $|[\bar{1}10]|$. Thus the two lattices are centred respectively on the positions O_N (origin of the normal lattice) and $O_T^1 = O_N + \frac{1}{2}[\bar{1}10]$ (origin of the lattice in the twin position). According to the authors this situation was chosen 'since it gives a normal packing arrangement for the molecules on both sides of the twin boundary'. The contribution of the N crystal to the potential energy of the molecules of the T crystal near such a twin boundary gives the following values for $-U_p^\circ/\varepsilon$

Molecule	O_T^1,	O_T^2,	C_T^1,	C_T^2,	O_T^3;
$-U_p^\circ/\varepsilon$	706,	239,	242,	31,	48.

Thus there is an important lack of balance between the values of U_p°/ε for two successive [110] rows in the crystal: $U_p^\circ/\varepsilon = -1000$ and -279, respectively, for rows 1 and 2 in Fig. 5. The total interaction energy for these rows is 70·38 kcal mol^{-1}, *i.e.* $7{\cdot}9 \times 10^{-5}$ erg cm^{-1}, taking into account that the period of the created interface corresponds in this case to a length (**a** + **b**). The resulting twin energy is $0{\cdot}47 \times 10^{-5}$ erg cm^{-1}.

So a highly kinked twin boundary as proposed in the Khoury–Dawson model seems to be less probable than the straight one, according to the higher twin energy, and to the important lack of balance in the energies outlined above. Furthermore, from our p.b.c. analysis, there is no reason for (110) to be an S face with its micro-facets developing in zone with the [001] direction. For these reasons we prefer in the sequel to work with the model of the straight (110) twin boundary.

6. Interaction energies in the dihedral angles near the (110) twin boundary

Let us consider first a molecule R_N placed in the reentrant angle near the twin boundary (Fig. 6). This molecule belongs to the N-crystal lattice, but, at the same time, occupies a lattice position of the T crystal. Its potential energy, in regard to all the molecules in the monomolecular layer of both crystals, corresponds to $U_p^\circ/\varepsilon = -601$ (-386 and -215 coming respectively from the crystals N and T). This means that in this particular site of the reentrant angle, the linkage of the molecule is at least as good as that of a molecule in a normal kink position (K_N in Fig. 2) for which $U_p^\circ/\varepsilon = -596$. The position of R_N is a permanent kink, from which the filling up of the $\langle 110\rangle$ rows of both N and T crystals starts spontaneously. So, as soon as a molecule is adsorbed in the R_N position, the successive molecules may add in the $\langle 110\rangle_{N,T}$ rows forming the reentrant angle, following the order indicated in Fig. 6, the influence of the reentrant angle decreasing sharply with the distance. Furthermore, a new molecule may adsorb in the R_N' position, before the $\langle 110\rangle_{N,T}$ rows are filled. Finally, if there is a very small supersaturation, these rows fill up normally and the permanent kink in the reentrant angle allows growth without any one or two-dimensional nucleation.

In the salient angle, near the twin boundary, the situation of a molecule such as S_N, for instance, is completely different from that of R_N (Fig. 6). The contributions to its potential energy are $U_p^\circ/\varepsilon = -210$ for the N crystal and $= -38$ for the T crystal. The total potential energy of S_N corresponds thus to $U_p^\circ/\varepsilon = -248$, a value even lower than that of a molecule normally adsorbed on a $\langle 110\rangle$ step such as A_N in Fig. 2 for which $U_p^\circ/\varepsilon = -425$. So, adsorption cannot take place on this site if there is not a complete row AB (or $A'B'$) of molecules to which S_N may join. If one of these rows exists the value U_p°/ε of S_N is then -420. In other words, the growth of the faces forming the salient angle cannot start at the top of this angle since an isolated molecule adsorbed in this position has a very high probability of desorption.

Up to now we have considered that the two (110) faces in contact had the same extension along the twin boundary (Fig. 6). This may be regarded as the final shape of the twin and the more probable one, whatever the initial stage of the twin formation may be.

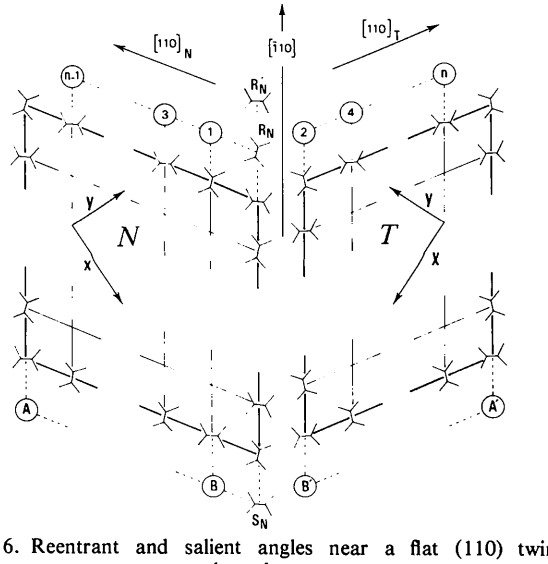

Fig. 6. Reentrant and salient angles near a flat (110) twin boundary.

Let us consider a twin boundary where the (110) face of the N crystal is more extended than its corresponding (110) face in the T crystal (Fig. 7). The discussion here is once more limited to the interaction energies within the monomolecular layer.

As may be seen in Fig. 7, there are two reentrant angles (R_1 and R_2) where growth may take place but not in the same conditions. The problem here is to find in what way these angles are filled by the growth units, taking into account their adhesion energies.

Among the different adsorption sites within the angle R_1, the site showing the largest probability of accepting a growth unit is R_{11} either when it corresponds to the positions O_T or C_T of the T lattice shown in Fig. 4; actually, for this site the contributions of the individuals N and T are the largest. The two cases being practically identical, we discuss the case where R_{11} is an O_T site. Looking for the different possibilities of finding a molecule adsorbed in unoccupied sites of the crystal we obtain the succession of the molecules $R_{11}\cdots R_{16}$ characterized by the following values of $-U_p^\circ/\varepsilon$:

molecule	R_{11}	R_{12}	R_{13}	R_{14}	R_{15}	R_{16}
$-U_p^\circ/\varepsilon$	766	638	793	619	611	746.

If we continue adding molecules, they turn out to place themselves first of all along the twin boundary or along the free edge of the T crystal; therefore, the angle R_1 is progressively filled with $[010]_T$ rows as displayed in Fig. 7. It is obvious that this filling up may be realized because the U_p°/ε values quoted exceed the corresponding value for a kink position. In other words the adsorption of the growth units is achieved spontaneously and the angle R_1 is unstable.

Applying the same reasoning to the angle R_2 we obtain the following succession of the adsorbed molecules $R_{21}\cdots R_{26}$ together with their respective values of $-U_p^\circ/\varepsilon$:

molecule	R_{21}	R_{22}	R_{23}	R_{24}	R_{25}	R_{26}
$-U_p^\circ/\varepsilon$	590	612	632	606	607	629.

Also in this case, the average value of the adhesion energy for the adsorbing molecules is higher than the corresponding value for a kink position. Nevertheless in this angle the adhesion energies of the molecules are weaker than in R_1 and its filling up is realized by means of $[100]_T$ rows. Summarizing, in both angles R_1 and R_2 the filling up is spontaneous, even at equilibrium, with a higher probability in R_1 than in R_2.

In order to determine the growth evolution in these angles, it is necessary to know the specific edge energies of all edges appearing in the twin at equilibrium. They may be obtained from the individual values displayed in Fig. 2. For $\langle 110\rangle$, [010], [100] and $\langle \bar{1}30\rangle$ these specific edge energies are respectively: 4·185, 3·98, 4·59 and $4{\cdot}36 \times 10^{-5}$ erg cm^{-1}.

Applying Wulff's (1901) theorem, it is then possible to calculate by means of these values the equilibrium form of a monomolecular layer lying on an infinite crystal. The corresponding plot is shown in Fig. 8. Obviously, the $\langle 110\rangle$ and [010] edges are well-developed whereas the [100] and $[\bar{1}30]$ edges have very short extents. In order to reach the equilibrium form of the three-dimensional crystal, it would be sufficient to multiply all the values of the specific edge energies by a constant $(10^8/d_{002})$, obtaining in this way the corresponding specific surface energies in erg cm^{-2}. The contributions of the end-packing energies can be neglected here; the error on the value of every surface energy is about 4% for $C_{36}H_{74}$, and decreases rapidly when the paraffinic chain-length increases.

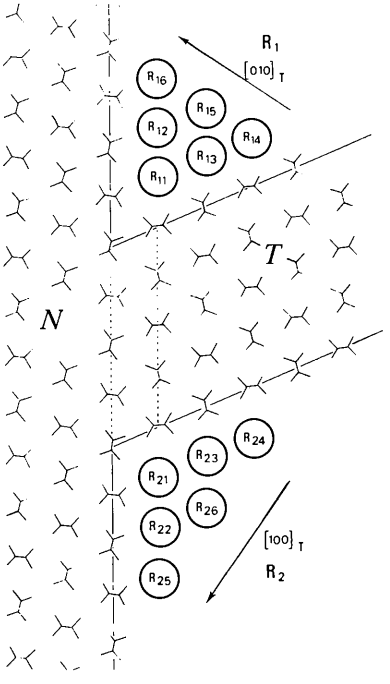

Fig. 7. First stages of the formation of a (110) twin boundary. Deposition sequence of the molecules in the reentrant angles R_1 and R_2.

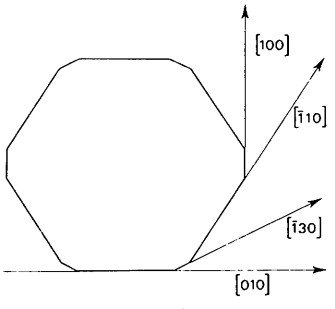

Fig. 8. Edges limiting the equilibrium form of a monomolecular layer adsorbed on an infinite (001) face.

From these considerations we deduce that the [010] ledges, at equilibrium, are stable and well-developed within the angle R_1. On the other hand, within R_2, the [100] ledges cannot exceed a certain length corresponding to the vanishing of the reentrant angle effect: in this case the monomolecular layer within R_2 will be limited by $\langle 110 \rangle$ ledges truncated by short [100] ledges.

If the bulk is slightly supersaturated the [100] and $\langle \bar{1}30 \rangle$ ledges vanish very rapidly. The [010] ledges vanish also, but less rapidly than the previous ones, and the final shape of the twin will contain only $\langle 110 \rangle$ ledges and will be elongated along the twin boundary (Dawson, 1952; Khoury, 1963).

7. Interaction energies along the (310) twin boundary

The (310) twin, which also exhibits dihedral reentrant and salient angles, was observed by Khoury (1963) on n-$C_{94}H_{190}$ crystals. Its occurrence frequency is, however, very low. According to the results of our p.b.c. analysis, (310) is an S face, with its edges running along the [001] direction and the interface between the two individuals of the twin is made of (110) and (100) microfacets alternating along the mean [$\bar{1}$30] direction (Fig. 9).

The molecules of the T crystal were generated from the molecules of the N crystal in the same way as for the (110)-twin law, the clockwise rotation here being 53°. Taking into account only the molecules inside a monomolecular layer, the potential energies of the molecules A, B, C and D near the twin boundary correspond respectively to $U_p^\circ/\varepsilon = -526, -214, -521, -220$. The calculated specific energy of the [$\bar{1}$30] edge is $\gamma_{[\bar{1}30]} = 4{\cdot}36 \times 10^{-5}$ erg cm^{-1}. The interaction energies with the N crystal of the [100] rows of the T crystal (Fig. 10), starting from the molecules A, B, C and D, correspond respectively to $U_p^\circ/\varepsilon = -590, -240, -586$ and -221. The sum of these quantities, which represents the interaction energy between the crystals T and N over a period $|[\bar{1}30]|$, corresponds to $U_p^\circ/\varepsilon = 1673$, *i.e.*, $7{\cdot}69 \times 10^{-5}$ erg cm^{-1}. It follows that the (310)-twin energy for a monomolecular layer is $1{\cdot}034 \times 10^{-5}$ erg cm^{-1}, a value about four times larger than the corresponding one for the (110)-twin law. These results are in good agreement with the experimental data: the occurrence frequency of the (310)-twin law is very low compared with that of the (110)-twin law.

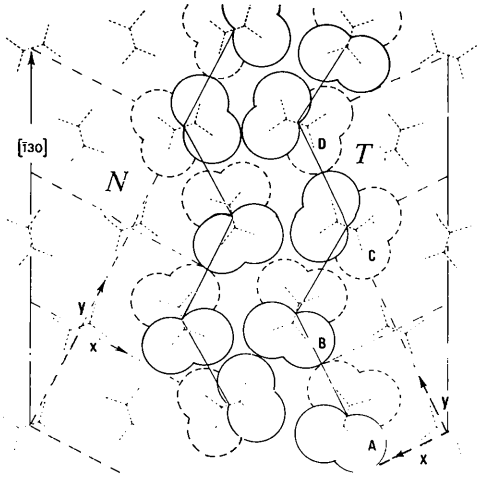

Fig. 9. (001) projection of a (310) twin boundary actually built up by (110) and (100) ledges.

8. Interaction energies in the dihedral angles near the (310) twin boundary

In the reentrant angle of this twin a molecule R_T (Fig. 10) has a potential energy corresponding to $U_p^\circ/\varepsilon = -435, -425, -427$ and -422, according as to whether the molecule R_T is of the type A, B, C or D. We can thus accept for R_T a mean value of -427. The contributions of each individual (N, T) on R_T are dependent on the site occupied by this molecule. For instance, if R_T is of type A, the contributions of the crystals N and T correspond respectively to $U_p^\circ/\varepsilon = -205$ and -230, whereas, if R_T is of type B these contributions correspond to $U_p^\circ/\varepsilon = -29$ and -396.

In any case the potential energy of R_T is practically the same as that corresponding to a normally adsorbed molecule along a $\langle 110 \rangle$ ledge (A_N in Fig. 2, for which $U_p^\circ/\varepsilon = -425$). Conversely, it is also much lower than the energy of a molecule in a kink site (K_N in Fig. 2, for which $U_p^\circ/\varepsilon = -596$). It follows that R_T is neither a permanent kink nor a preferential growth site in which growth can take place spontaneously. The reentrant angle has almost no influence on the growth kinetics of the $(110)_{N,T}$ faces by which it is made.

With the same reasoning, it can be shown that a molecule S_N in the salient angle has a potential energy corresponding to a mean value of $U_p^\circ/\varepsilon = -394$. This

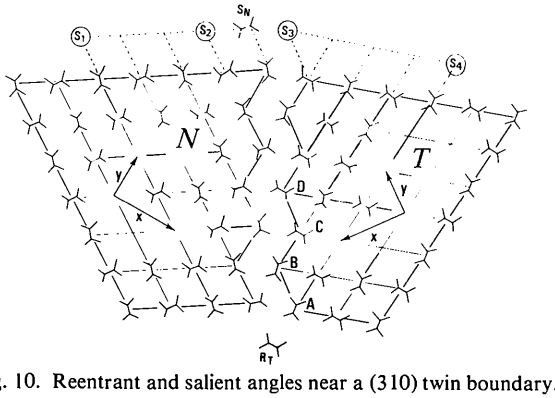

Fig. 10. Reentrant and salient angles near a (310) twin boundary.

molecule can adsorb only if the rows S_1S_2 or S_3S_4 already exist. As for the analogous case in the (110)-twin law, growth cannot start from the top of this angle. The calculations here are also in good agreement with the experimental data of Khoury (1963) who never observed special growth directions on the (310)-twinned crystals.

9. Conclusion

The (110) and (310)-twin energies of orthorhombic hexatriacontane crystals, calculated with a Lennard-Jones 6–12 potential, can be extrapolated to all the long-chain paraffins of the orthorhombic series as a function of the number of C atoms in the chains. The results given above depend only on the potential function and on the twin boundary models.

In the case of the (110) twin law, the interaction energies across the twin boundary have been calculated considering interfaces either completely flat or corrugated to the highest possible extent. From our p.b.c. analysis it emerges that the former is the more probable. Near the kinks of the interface, there must be a certain displacement of the molecules in order to compensate for the lack of balance of the molecular interaction energies. The real value of the (110)-twin energy is thus probably only a little higher than that calculated for a completely flat twin boundary. As for the (310)-twin law, its four-times-higher twin energy explains its low occurrence frequency.

If we consider the growth of twinned crystals, the salient angles formed by the two individuals are of no effect on the growth kinetics since all the adsorbed molecules in these angles have lower adhesion energies than a molecule adsorbed in a half-crystal position. On the other hand, the molecules adsorbing in some re-entrant angles, built up by faces of the same (*hkl*), may have near the twin boundary adhesion energies higher than a molecule in a normal kink. In this case, the re-entrant angles act as permanent kinks and during the growth there is an elongation of the crystals along the direction of the twin boundaries. If the reentrant angles are made up by faces of different (*hkl*), they disappear by formation of new facets. These facets can remain or disappear from the growth form according to the growth conditions.

Finally, the results quoted in this study were obtained with the aid of calculations valid in the crystal–vapour system; the resulting growth morphologies were compared with that of twinned crystals grown from solution. The agreement is good and we may conclude that the adsorption of the solvents on the paraffin crystals does not change significantly the equilibrium form of the crystals, keeping nearly constant the ratios between the different surface, edge or twin energies.

References

AMELINCKX, S. (1956*a*). *Acta Cryst.* **9**, 16–23.

AMELINCKX, S. (1956*b*). *Acta Cryst.* **9**, 217–224.

AQUILANO, D. (1977). *J. Cryst. Growth*, **37**, 215–228.

BOISTELLE, R. & AQUILANO, D. (1977). *Acta Cryst.* A**33**, 642–648.

BOISTELLE, R. & DOUSSOULIN, A. (1976). *J. Cryst. Growth*, **36**, 335–352.

DAWSON, I. M. (1952). *Proc. R. Soc. London Ser. A*, **214**, 72–79.

FRANK, E. C. (1949). *Discuss. Faraday Soc.* **5**, 48 and 186.

HARTMAN, P. (1956). *Z. Kristallogr.* **107**, 225–237.

HARTMAN, P. & PERDOK, W. G. (1955). *Acta Cryst.* **8**, 49–52.

KELLER, A. (1961). *Philos. Mag.* **6**, 329–335.

KHOURY, F. (1963). *J. Appl. Phys.* **34**, 73–79.

MADSEN, H. E. L. (1978). *J. Cryst. Growth*. To be published.

MADSEN, H. E. L. & BOISTELLE, R. (1976). *Acta Cryst.* A**32**, 828–831.

NYBURG, S. C. & POTWOROWSKI, J. A. (1973). *Acta Cryst.* B**29**, 347–352.

SMITH, A. E. (1953). *J. Chem. Phys.* **21**, 2229–2231.

STRANSKI, I. N. (1949). *Discuss. Faraday Soc.* **5**, 69 and 75.

TEARE, P. W. (1959). *Acta Cryst.* **12**, 294–300.

UBBELHODE, A. R. (1938). *Trans. Faraday Soc.* **34**, 282–299.

WULFF, G. (1901). *Z. Kristallogr.* **34**, 449–530.